Journal of
Mechanics of
Materials and Structures

A HIGHER-ORDER THEORY FOR CRACK GROWTH IN FIBER-METAL LAMINATES UNDER GENERALIZED PLANE-STRESS CONDITIONS

Xijia Wu, Zhong Zhang and J. Laliberté

Volume 1, Nº 3 March 2006

mathematical sciences publishers

JOURNAL OF MECHANICS OF MATERIALS AND STRUCTURES
Vol. 1, No. 3, 2006

A HIGHER-ORDER THEORY FOR CRACK GROWTH IN FIBER-METAL LAMINATES UNDER GENERALIZED PLANE-STRESS CONDITIONS

XIJIA WU, ZHONG ZHANG AND J. LALIBERTÉ

Fiber-metal laminates (FML) are hybrid materials that consist of alternating layers of metal and fiber-reinforced prepreg. The classical plane-stress theory has difficulty in dealing with the fatigue fracture of such materials where the crack only grows in the metal layers, while the prepreg layers remain intact. In this paper, a new theoretical treatment is given to FML under generalized plane-stress conditions. The new theory introduces a harmonic anti-plane-stress potential p to describe the interlaminar stresses near the crack tips and the "bridging" effect of the unbroken fibers along the crack wakes. An analytical solution is derived for GLARE-3 (3/2) containing collinear cracks with length $2a_0$ (the initial crack length) in the prepreg and length $2a$ in the aluminum layer. The effective stress intensity factor is obtained in a closed form, and the theoretical prediction is compared with the experimental behavior obtained from fatigue crack growth testing of center-notched specimens.

1. Introduction

Fiber-metal laminates (FML) consisting of alternating layers of aluminum and fiber-reinforced prepreg are being considered as a potential alternative to replace traditional aluminum alloys for more light-weight and damage tolerant aerospace structural applications [Gunnink et al. 1982]. FML have excellent fatigue crack growth resistance plus improved impact and corrosion resistances because the fiber reinforcement plays a role in crack bridging and also insulates the inner metal from any corrosive species. It has been recognized that the damage tolerance characteristics of FML are largely attributed to the load transfer mechanism via interfacial shear stresses from the cracked aluminum layers to fiber-reinforced (unbroken) prepregs [Gunnink et al. 1982; Roebroeks 1994]. Regarding the fiber-bridging effect, Marissen [1988] assumed that a constant "bridging stress" exists in the fibers along the crack wake. Guo and Wu [1999] offered a numerical method to derive the

Keywords: fiber-metal laminate, stress intensity factor.

"bridging stress" based on the displacement condition at the boundary of delamination. Their treatment rests on two assumptions: (i) each fiber within the delamination region is individually under uniform tension, and (ii) the displacement profile at the delamination boundary is equal to the crack opening displacement along the crack wake. The error associated with the assumed displacement condition would be proportional to the size of delamination (that is, $\Delta v \propto \varepsilon f(x)$, where $f(x)$ is the delamination boundary away from the crack line $y = 0$), if a constant strain existed across the region. The aforementioned theoretical treatments attempted to patch the shortcomings of the classical crack mechanics for monolithic materials, but they were not derived from the stress equilibrium and compatibility equations of elasticity. For laminated materials, the existence of parallel cracks of different length in different layers poses a significant challenge to the classical two-dimensional theories dealing with plates and laminates, and the general solution has not been found.

Traditionally, composite materials are considered as homogeneous and anisotropic materials and hence are solved with the classical theory [Tsai and Hahn 1980; Whitney 1987; Ashbee 1993], where the anti-plane shear stresses are absent because of the simplification. Except for some 3D or quasi-3D numerical methods—such as the finite element method, the hybrid and displacement superposition method [Pagano 1978; Iarve and Pagano 2001]—that could be used to describe cracks in FML where layer-to-layer interaction cannot be ignored, there is no analytical theory to formulate stresses in cracked FML. It is the intention of this paper to present such a theory.

A higher-order theory has been developed for generalized plane-stress states in isotropic materials with the introduction of two conjugated harmonic stress potentials for anti-plane stresses by the requirement of 3D strain compatibility [Wu and Cheng 1999]. This theory is now extended to FML whereby the interlaminar stress interaction is reduced to equivalent body forces. As an example, the boundary-value problem of fatigue crack growth in GLARE-3 (3/2) is solved, using the complex variable method. The effective stress intensity factor of a crack in FML, propagating only in the aluminum layers, is obtained in a closed form and the prediction is then compared with the experimental behavior observed from fatigue crack growth testing of center-notched specimens.

2. The theory of FML

Consider a typical fiber-metal laminate, which consists of alternating metal (isotropic) and prepreg (orthotropic) layers. The configuration of GLARE-3 (3/2) is shown in Figure 1. The reference coordinate system is also given in 1 by way of

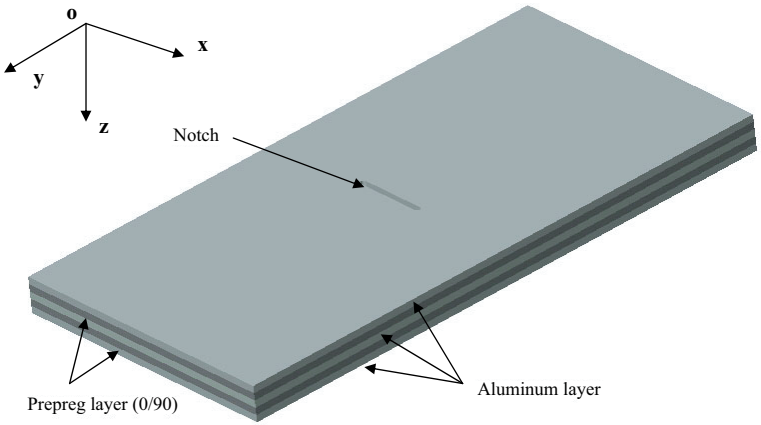

Figure 1. Schematic configuration of GLARE-3 (3/2) consisting of three layers of 2024-T3 aluminum alloy and two layers of glass fiber-epoxy prepreg.

describing the problem. For the panel, the thickness of the laminate is small compared to the planar dimensions. The body forces are ignored and the stress normal to the laminate, σ_z, is zero. In the following, we shall derive the stress formulation for metal and prepreg layers separately and then consider their interactions by the requirement of displacement continuity across the interface.

2.1. ***The metal layer.*** Under the generalized plane stress condition, the stress equilibrium in the metal layer can be expressed as

$$\frac{\partial \sigma_x}{\partial x} + \frac{\partial \tau_{xy}}{\partial y} + \frac{\partial \tau_{xz}}{\partial z} = 0, \tag{1a}$$

$$\frac{\partial \tau_{xy}}{\partial x} + \frac{\partial \sigma_y}{\partial y} + \frac{\partial \tau_{yz}}{\partial z} = 0, \tag{1b}$$

$$\frac{\partial \tau_{xz}}{\partial x} + \frac{\partial \tau_{yz}}{\partial y} = 0. \tag{1c}$$

It has been shown that the three-dimensional stress equilibrium and strain compatibility conditions can be all met when the in-plane and anti-plane shear stresses are expressed as [Wu and Cheng 1999]

$$\sigma_x = \frac{\partial^2 \Psi}{\partial y^2} + p, \qquad \sigma_y = \frac{\partial^2 \Psi}{\partial x^2} + p, \qquad \tau_{xy} = -\frac{\partial^2 \Psi}{\partial x\, \partial y}, \tag{2}$$

$$\tau_{xz} = -z\frac{\partial p}{\partial x} = -z\frac{\partial q}{\partial y}, \qquad \tau_{yz} = -z\frac{\partial p}{\partial y} = z\frac{\partial q}{\partial x}, \tag{3}$$

where Ψ is a bi-harmonic function ($\nabla^4\Psi = 0$), p and q are conjugated harmonic functions ($\nabla^2 p = 0$ and $\nabla^2 q = 0$, satisfying the Cauchy–Riemann condition).

For each individual layer, the neutral plane ($z = 0$) is set at either the free surface, for a surface metal layer, or the median plane for a middle layer. Therefore, the free surface is truly free of any anti-plane shear traction. Alternatively, the laminate can also be viewed as a portion of periodical stacking of the constituent lamina, in which the surface layer becomes an inner layer with twice the thickness. When the lay-up is symmetrical, as in GLARE 3, the net anti-plane shear stress across the laminate is zero, and the laminate is under the generalized plane-stress condition. When the lay-up is asymmetrical, a coupled bending is induced, because the net anti-plane shear is not always zero. Here we consider only the former case. For that, the inter-laminar shear stresses at the interfaces of metal/prepreg can be obtained from Equation (3) as

$$\tau_{xz}^i = \mp\frac{h_i}{2}\frac{\partial p_i}{\partial x}, \qquad \tau_{yz}^i = \mp\frac{h_i}{2}\frac{\partial p_i}{\partial y}, \qquad i = 1, 3, 5, \ldots, \tag{4}$$

where h_i is the thickness of the i-th layer. The detailed lay-up is shown in Figure 2 and the sign convention is observed accordingly.

2.2. ***The prepreg layer.*** For a prepreg layer between metal layers ($i = 2, 4, 6, \ldots$), the action of the inter-laminar shear stresses would produce an effect equivalent to that of the in-plane body forces, as defined by

$$X_i = -\frac{\tau_{xz}^{i+1} - \tau_{xz}^{i-1}}{h_i} = -\frac{1}{2h_i}\frac{\partial}{\partial x}\left(h_{i+1}p_{i+1} + h_{i-1}p_{i-1}\right) = -\frac{\partial U}{\partial x}, \tag{5a}$$

$$Y_i = -\frac{\tau_{yz}^{i+1} - \tau_{yz}^{i-1}}{h_i} = -\frac{1}{2h_i}\frac{\partial}{\partial y}\left(h_{i+1}p_{i+1} + h_{i-1}p_{i-1}\right) = -\frac{\partial U}{\partial y}, \tag{5b}$$

where U is defined as the equivalent body-force potential:

$$U = \frac{1}{2h_i}\left(h_{i+1}p_{i+1} + h_{i-1}p_{i-1}\right). \tag{5c}$$

Therefore, the equilibrium equations for the prepreg reduce to

$$\frac{\partial \sigma_x}{\partial x} + \frac{\partial \tau_{xy}}{\partial y} + X_i = 0, \tag{6a}$$

$$\frac{\partial \tau_{xy}}{\partial x} + \frac{\partial \sigma_y}{\partial y} + Y_i = 0. \tag{6b}$$

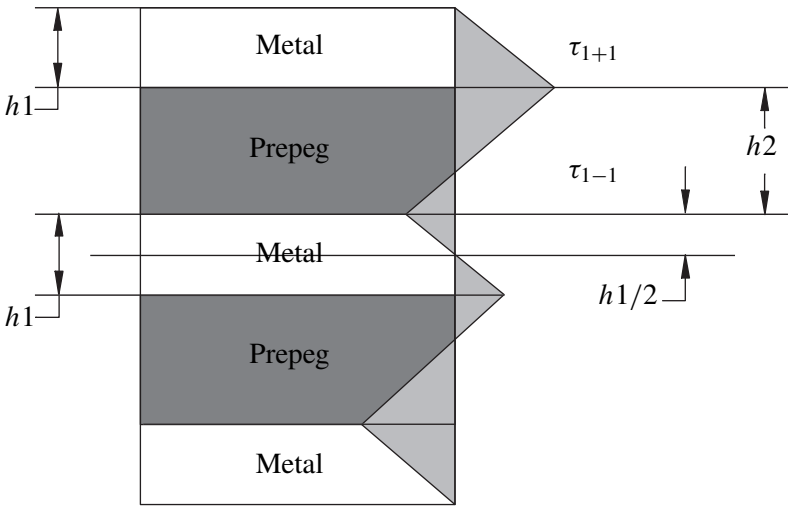

Figure 2. Schematic of inter-laminar shear stress distribution through the thickness of an FML.

By satisfying the equilibrium conditions, the in-plane stresses in a prepreg can be obtained as

$$\sigma_x = \frac{\partial^2 F}{\partial y^2} + U, \qquad \sigma_y = \frac{\partial^2 F}{\partial x^2} + U, \qquad \tau_{xy} = -\frac{\partial^2 F}{\partial x\, \partial y}, \tag{7}$$

where F is the stress potential of the prepreg and should satisfy the compatibility condition for an orthotropic material [Lekhnitskiĭ 1981]:

$$a_{22}\frac{\partial^4 F}{\partial x^4} + (a_{66} + 2a_{12})\frac{\partial^4 F}{\partial x^2\, \partial y^2} + a_{11}\frac{\partial^4 F}{\partial y^4} = -(a_{22} + a_{12})\frac{\partial^2 U}{\partial x^2} - (a_{11} + a_{12})\frac{\partial^2 U}{\partial y^2}, \tag{8}$$

where a_{ij} are the compliance coefficients of the prepreg.

For FML of symmetrical layout, the anti-plane shear stresses counteract each other across the entire thickness of the laminate such that the net result is zero. Thus, the stress-state of FML, as defined by the stress functions Ψ, F, U, p and q, falls into the category of the generalized plane stress.

In summary, the stresses in a metal (isotropic) layer can be obtained from the stress function Ψ and either of the conjugated harmonic functions p and q; the stresses in a prepreg (orthotropic) layer can be obtained from the stress functions F and U. The inter-laminar stresses can be calculated using Equation (4). These stress potentials, when satisfying the necessary compatibility conditions, should lead to a complete description of the stresses in the laminate. By the theorem of unique solution of elasticity, the stress potentials should represent the true stress-state of the laminate under a given generalized plane-stress condition. The problem, then, reduces to finding stress functions (or potentials) that meet the boundary-value conditions of the particular loading configuration. The mathematical approach to seeking such solutions is discussed along with the presentation of solving a practical case of fatigue crack growth in GLARE-3 (3/2) in the section below.

3. The complex variable solution for GLARE-3 containing a crack

Consider a GLARE-3 (3/2) panel containing central collinear cracks of length $2a$ in the aluminum and $2a_0$in the prepreg. The panel is remotely subjected to uniform tension, as shown schematically in Figure 3. The crack in the prepreg represents

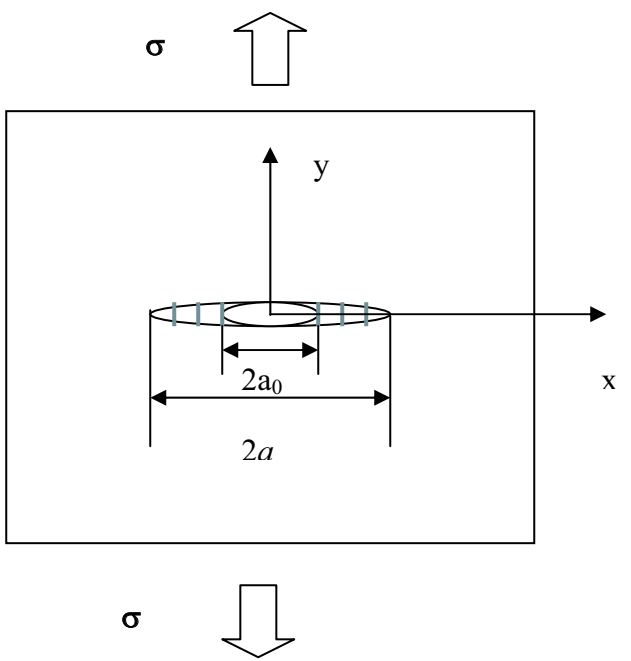

Figure 3. Schematic of a FML panel containing a center-located crack: a_0 is the half-length of the initial through-the-thickness crack; a is the half-length of the crack in the metal layer.

the initial notch, the ones in the metal layers extend to the current length a due to fatigue crack growth. As such, the crack wakes in the region $[a_0, a]$ are bridged with unbroken fibers. The aluminum layers are 2024-T3 sheets, which are considered to be isotropic materials. The prepreg layers in GLARE-3 have equal volume fraction of 0°/90° cross-ply glass fibers, and therefore are also treated as a quasi- isotropic material, for simplicity. This greatly reduces the complexity of the problem and allows one set of stress potential functions to be used for both aluminum and prepreg in GLARE-3, as detailed below. For other FML with anisotropic prepregs, the solution has to be obtained by solving Equation (8).

First, the Westergaard function is adopted as the in-plane stress potential ψ, as defined by

$$\psi = \operatorname{Re} \tilde{\tilde{Z}}(\xi) + y \operatorname{Im} \tilde{Z}(\xi), \tag{9}$$

where $\xi = x + iy$ is the complex coordinate variable and

$$\begin{aligned} \tilde{Z} &= \int Z(\xi)\, d\xi, \\ \tilde{\tilde{Z}} &= \int \tilde{Z}(\xi)\, d\xi = \iint Z(\xi)\, d\xi\, d\xi. \end{aligned} \tag{10}$$

Then, a new analytic function $\chi(\xi)$ is introduced to express the anti-plane shear stress potential p as

$$2p = \chi(\xi) + \bar{\chi}(\bar{\xi}) = \varphi'(\xi) + \bar{\varphi}'(\bar{\xi}), \tag{11}$$

where $\bar{\xi}$ denotes the conjugate of ξ, and the same meaning also applies to complex functions.

Hence, according to Equations (2) and (3), the stress components can be obtained as

$$\begin{aligned} \sigma_x + \sigma_y &= 2 \operatorname{Re}\left[Z(\xi) + \chi(\xi)\right], \\ \sigma_y - \sigma_x + i2\tau_{xy} &= -i2yZ'(\xi), \\ \tau_{xz} + i\tau_{yz} &= \mp \frac{h}{2} \bar{\chi}'(\bar{\xi}). \end{aligned} \tag{12}$$

The displacements (at $z = 0$) can be obtained as

$$2G(u + iv) = \frac{2}{1+\mu} \tilde{Z}(\xi) - \operatorname{Re} \tilde{Z}(\xi) - iy\bar{Z}(\bar{\xi}) + \frac{1-\mu}{1+\mu} \varphi(\xi). \tag{13}$$

Because of symmetry, the solution for the half plane $x > 0$ can be tentatively represented by the following functions:

$$Z(\xi) = \frac{A\xi}{\sqrt{\xi^2 - a^2}}, \qquad \chi(\xi) = \frac{B}{\sqrt{\xi - a}}, \tag{14}$$

where A and B are constants to be determined by the stress boundary conditions and displacement compatibility conditions.

Substituting Equation (14) into Equations (12) and (13), we obtain the in-plane stresses as

$$\sigma_x = \frac{\partial^2 \psi}{\partial y^2} + p = \operatorname{Re}\left[Z(\xi) + \chi(\xi)\right] - y \operatorname{Im} Z'(\xi),$$

$$\sigma_y = \frac{\partial^2 \psi}{\partial x^2} + p = \operatorname{Re}\left[Z(\xi) + \chi(\xi)\right] + y \operatorname{Im} Z'(\xi), \tag{15}$$

$$\tau_{xy} = -y \operatorname{Re} Z'(\xi),$$

and the displacements as

$$u = \frac{1}{2G}\left(\frac{1-\mu}{1+\mu} \operatorname{Re}\left[\tilde{Z}(\xi) + \varphi(\xi)\right] - y \operatorname{Im} Z(\xi)\right), \tag{16a}$$

$$v = \frac{1}{2G}\left(\frac{2}{1+\mu} \operatorname{Im} \tilde{Z}(\xi) - y \operatorname{Re} Z(\xi) + \frac{1-\mu}{1+\mu} \operatorname{Im} \varphi(\xi)\right). \tag{16b}$$

It is easy to verify that the crack surface condition, that is, $\tau_{xy} = \sigma_y = 0$, at $y = 0$, $|x| < a$, is satisfied and the displacement v along the line of $(x > a,\ y = 0)$ is zero. To satisfy the remote stress condition, $A = \sigma_\infty$. These stress/displacement formulations will be used to deal with two cracks in an FML: one crack of length $2a_0$ in the prepreg and one of length $2a$ in the aluminum.

For displacement continuity, it is assumed that the crack opening displacements at the center of both cracks in metal and prepreg are equal, due to the perfect bonding condition. Mathematically, this condition can be expressed as: $v^{(1)} = v^{(2)}$ at the point $(x = 0,\ y = 0)$. In the rest of the plane of the interface, displacement discontinuities or sliding may occur, particularly around the crack tips. The assumed condition is a simplification for the convenience of deriving a closed-form solution as shown in the following, yet it adheres to the fact that delamination does not occur at the center point. The above description is only a two-dimensional simplification of the delamination problem in a real case, a complete description of which would have to be based on a 3D theory.

From Equation (16b), the crack-center opening displacements in the metal (with a crack of half-length a) and prepreg (with a crack of half-length a_0) can be obtained, respectively, as

$$\begin{aligned} v^{(1)} &= \frac{1}{G_1}\left(\frac{A^{(1)}a}{1+\mu} + \frac{(1-\mu)B^{(1)}\sqrt{a}}{1+\mu}\right), \\ v^{(2)} &= \frac{1}{G_2}\left(\frac{A^{(2)}a_0}{1+\mu} + \frac{(1-\mu)B^{(2)}\sqrt{a_0}}{1+\mu}\right), \end{aligned} \tag{17}$$

where $v^{(1)}$ and $v^{(2)}$ are the displacements in the y direction for the metal and prepreg layers. $A^{(1)}$, $B^{(1)}$ and $A^{(2)}$, $B^{(2)}$ are constants for metal and prepreg layers, respectively. Since both layers are subjected to remote uniform tension, $A^{(1)} = \sigma^{(1)}$ and $A^{(2)} = \sigma^{(2)}$, where $\sigma^{(1)}$ and $\sigma^{(2)}$ are the remote stresses in the metal and prepreg layer, respectively. Then, only the constants $B^{(1)}$ and $B^{(2)}$ need to be determined to complete the solution.

There are two stress singularity points in the FML containing a fiber-bridged crack—one at $x = a_0$ and the other at $x = a$—which may cause local delamination due to incompatibility. This has indeed been observed in numerous experiments. At remote locations, however, it is believed that the bonding between the prepreg and the metal layers should remain intact such that the antiplane shear stresses are continuous across the interface. Thus, at the interface between the surface metal layer and an immediate inner prepreg layer, it should hold that

$$-h_1\bar{\chi}_1'(\bar{\xi}) = \frac{h_2}{2}\bar{\chi}_2'(\bar{\xi}), \qquad (\xi \to \infty), \tag{18}$$

where h_1 and h_2 are the thickness of the surface metal layer and the immediate prepreg layer, respectively. Equation (18) will hold true when $r = |\xi| \gg a_0$ and a, only if

$$2h_1B^{(1)} = -h_2B^{(2)}. \tag{19}$$

Then, by solving the displacement continuity condition at the crack center, that is, $v^{(1)} = v^{(2)}$ (at $x = 0$, $y = 0$), with the substitution of Equation (19) into Equation (17), we obtain

$$B^{(1)} = \frac{1}{1-\mu}\frac{A^{(2)}a_0 - \frac{G_2}{G_1}A^{(1)}a}{\frac{G_2}{G_1}\sqrt{a} + 2\frac{h_1}{h_2}\sqrt{a_0}} = -\frac{h_2}{2h_1}B^{(2)}. \tag{20}$$

We note here that the displacement continuity condition imposed at the crack-center is obviously an approximation of the more complicated interfacial continuity/discontinuity conditions around the crack in the real laminates. However, the major mechanical characteristics of the simplified condition agree with the real case, as elucidated in a later section.

From stress expression, Equation (15), the stress intensity factor in the metal layer can be obtained as:

$$K_{\text{eff}} = \lim_{\substack{x_1 \to 0 \\ y=0}} \sqrt{2\pi x_1}\sigma_y^{(1)} = K_\infty^{(1)} - \frac{\sqrt{2}}{1-\mu} \frac{K_\infty^{(1)} - \frac{G_1}{G_2}\sqrt{\frac{a_0}{a}} K_\infty^{(2)}}{1 + 2\frac{G_1 h_1}{G_2 h_2}\sqrt{\frac{a_0}{a}}}, \tag{21}$$

where, $x_1 = x - a$, and

$$K_\infty^{(1)} = A^{(1)}\sqrt{\pi a} = \sigma_\infty^{(1)}\sqrt{\pi a}, \qquad K_\infty^{(2)} = A^{(2)}\sqrt{\pi a_0} = \sigma_\infty^{(2)}\sqrt{\pi a_0}.$$

$\sigma_\infty^{(1)}$ and $\sigma_\infty^{(2)}$ are the remote stresses in the metal layer and prepreg layer.

4. Experiment

GLARE-3 3/2 specimens, which consist of three sheets of 2024-T3 aluminum alloy (0.3 mm thick) and two layers of glass/epoxy prepreg (0.25 mm thick) with a stacking sequence of (0°/90°), were machined (water-jet cut) in the form of center-crack tension specimen (CCT) configuration. The specimen has a length of 300 mm in the loading direction, a width of 100 mm and it contains a 24 mm long central notch with a notch root radius of 0.2 mm. The total thickness of the specimen is 1.4 mm. Fatigue crack growth rate testing was performed according to the ASTM-E647 standard. The testing was conducted at room temperature using a computer-controlled MTS servohydraulic testing machine under constant amplitude sinusoid loading with a frequency of 5 Hz and stress ratio $R = 0.1$. The crack length was measured using a traveling microscope (±0.01 mm). Fatigue testing was automatically stopped at a predetermined cycle interval to take measurements of the half-crack length on both sides of the specimen. An a-N curve is shown in Figure 4 (a). Details of the testing program were reported elsewhere [Zhang et al. 2002].

5. Discussion

Fatigue crack growth in FML has been investigated by many researchers, using semi-empirical approaches [Marissen 1988], experimental methods [Ritchie et al. 1989] and numerical methods [Guo and Wu 1998]. All these treatments used the concept of *bridging stress* to account for the reduction of stress intensity factor in FML, but it is empirically introduced. According to the present higher-order theory, it is the interlaminar shear stress that provides the bridging effect, as opposed to the in-plane "bridging stress" acting along the crack wake. The existence of these anti-plane shear stresses modifies the in-plane stresses through the interaction of stress potentials, as expressed in Equations (2) and (3). As a result, the stress intensity factor of the crack in the metal layer is changed, as shown in Equation (21), in

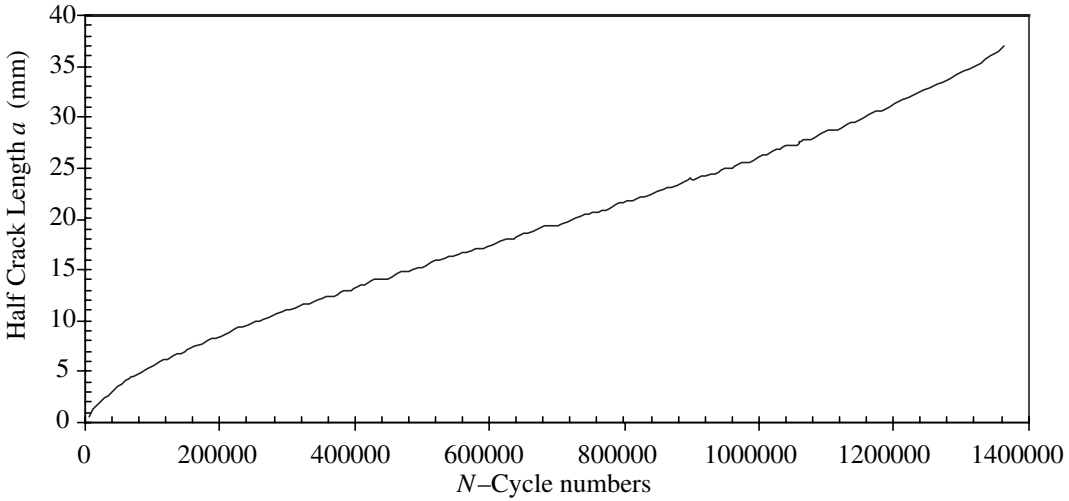

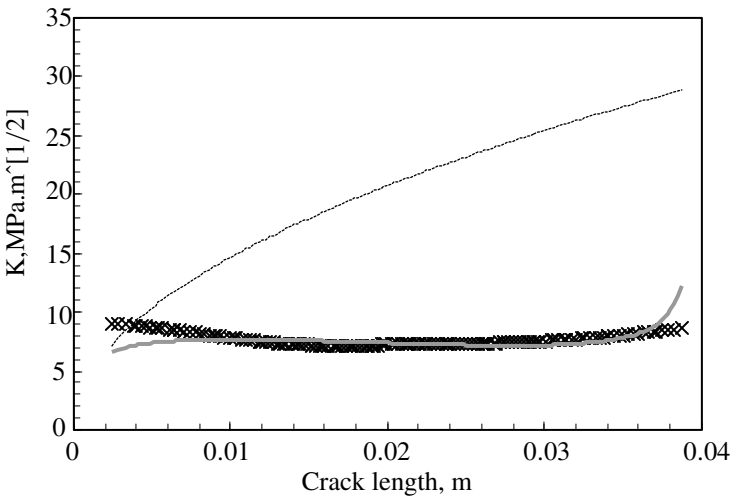

Figure 4. (a) Measured crack length as a function of fatigue cycle number; (b) comparison of the theoretical stress intensity factors with the experimental values: thin black line indicates monolithic K; thick black line shows FML-K; black X's indicate experimental values.

comparison with the solution for monolithic materials. Apparently, (21) can be broken into two parts, as

$$K_{\text{eff}} = K_m - K_{br}, \tag{22}$$

where K_m is the apparent stress intensity factor as if in the monolithic metal, and K_{br} is the stress intensity reduction due to fiber-bridging, as defined by

$$K_{br} = \frac{\sqrt{2}}{1-\mu} \frac{K_\infty^{(1)} - \frac{G_1}{G_2}\sqrt{\frac{a_0}{a}} K_\infty^{(2)}}{1 + 2\frac{G_1 h_1}{G_2 h_2}\sqrt{\frac{a_0}{a}}}. \tag{23}$$

Equation (22) bears a physical meaning similar to that perceived by other researchers, but only K_{br} is derived from anti-plane stresses and is explicitly expressed in Equation (23).

From the a-N curve, Figure 4 (a), fatigue crack growth rates can be evaluated. The effective stress intensity factors in the FML are thus found as compared with the metal fatigue crack growth behavior, that is, from the da/dN versus ΔK relationship, assuming that the fatigue crack, propagating in the aluminum alloy layer of an FML, experiences the same stress intensity at the same growth rate as it would were it propagating in the monolithic alloy alone. For the finite panel specimen configuration, a correction was made to Equation (21), replacing $K_\infty^{(1)}$ with

$$K_\infty^{(1)} \sqrt{\sec \frac{\pi a}{W}},$$

where W is the width of the specimen, to account for the effect of finite width.

In matching (21) with the real case, the value of a_0 has to be adjusted to account for the effect of bluntness of the initial machine notch in the specimen. Note that fatigue precracking in this case would only sharpen the metal crack but not the prepreg crack (notch). The comparison of (21) with the evaluated ΔK is shown in Figure 4 (b). The elastic properties of the FML, as input to the calculation, are: $G_1 = 27.7$ GPa, $h_1 = 0.3$ mm, for aluminum; and $G_2 = 5.6$ GPa, $h_2 = 0.25$ mm, for prepreg. The stress intensity factor of a crack in an infinite monolithic aluminum sheet is also shown in the figure for comparison purposes. It may be seen that a crack without fiber-bridging exhibits very high stress intensities as the crack grows, while the one in the FML tends to level off to a fairly constant value until the very end of the panel. Excellent agreement between the theoretical and experimental values can be found for the FML over 90% of crack growth range, except in the initial stage where the crack is perhaps under the influence of the notch plasticity.

To check the compatibility conditions at the interface, the difference between the displacements in the aluminum and the prepreg, $v_1 - v_2$, is calculated and mapped onto the panel plane (the x-y plane), as shown in Figure 5. We see that there is a discernible region of discontinuity, with a maximum occurring at $x = a_0$ (the tip of

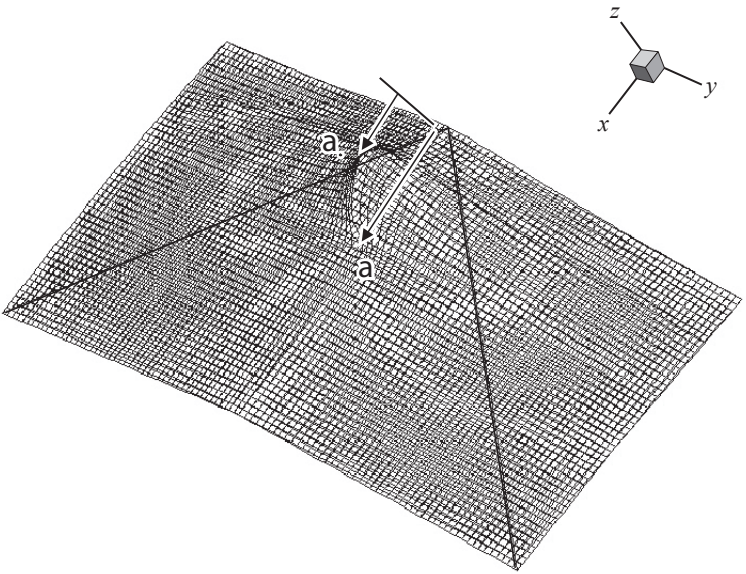

Figure 5. A map of displacement discontinuity at the interface between metal and prepreg layers. $X - Y$ represent the panel plane and Z represents the absolute value of $v_1 - v_2$.

the prepreg crack). This displacement discontinuity region actually corresponds to the shape of the delamination region rather well, as observed in the FML specimens both in our testing program and in others [Guo and Wu 1998]. It should be understood that the delamination problem in the present context within the framework of 2D elasticity is depicted as interfacial sliding, that is, relative in-plane displacement, as shown in Figure 5. Therefore, the criterion of delamination may be defined by how much the delta sliding can be accommodated by the gluing agent, which is determined by the physical properties of the interface. Such properties can be called the interfacial delamination resistance. Beyond that, interfacial breaking may occur, and thus physical delamination occurs. However, descriptions of the physical delamination process are beyond the scope of the theory of elasticity.

In summary, a higher-order laminate plate theory has been developed for fiber-metal laminates that consist of alternating metal and fiber-reinforced prepreg layers. The theory is an extension of the previous higher-order theory for generalized plane-stress problems of isotropic materials, which employs two harmonic anti-plane stress potentials, p and q, in addition to the bi-harmonic plane stress potential. When the displacement compatibility condition is set at the interlaminar interface, these anti-plane stress potentials play the role of load transfer between adjacent layers, particularly when one of them contains a crack. By taking advantage of

the complex variable method that has been developed and matured for monolithic isotropic materials [Muskhelishvili 1953; Lekhnitskiĭ 1981], one can easily extend the complex variable treatment, with the inclusion of an additional analytical function for the anti-plane stress potential to multi-layered bodies, as shown in the previous section. As an example, one mathematical solution is presented in this paper for GLARE-3 containing a fatigue crack, to show the application of the theory to practical problems.

6. Conclusion

1. A higher-order lamination theory has been developed for the plane-stress elasticity of fiber-metal laminates. The new theory employs anti-plane stress potentials to take into consideration possible interlaminar interactions, particularly when defects exist in certain layers, which tend to break the compatibility with the adjacent lamina. In this case, the anti-plane stress potentials produce an additional in-plane stress component that modifies the original (by the classical theory) stress state to re-establish the strain/displacement compatibility.
2. The complex variable representation of the plane-stress problem is modified to include the anti-plane shear stress function and a solution is derived for GLARE-3 (3/2) containing a fiber-bridged fatigue crack.
3. An effective stress intensity factor for GLARE-3 (3/2) is derived in closed form, which agrees with the test results, provided that the initial notch effect for the specimen is appropriately corrected.

Acknowledgment

The work was done under the NRC-IAR, research code 46_QJ0_18, with partial financial support from Bombardier Aerospace.

References

[Ashbee 1993] K. H. G. Ashbee, *Fundamental principles of fiber reinforced composites*, Technomic, Lancaster, PA, 1993.

[Gunnink et al. 1982] J. W. Gunnink, L. B. Vogelesang, and J. Schijve, "Application of a new material (ARALL) in aircraft structures", pp. 990–1000 in *Proc. 13th Congress of the International Council of the Aeronautical Sciences (ICAS)*, Seattle, WA, 1982.

[Guo and Wu 1998] Y. J. Guo and X. R. Wu, "A theoretical model for predicting fatigue crack growth rates in fibre-reinforced metal laminates", *Fatigue Fract. Eng. Mater. Struct.* **21**:9 (1998), 1133–1145.

[Guo and Wu 1999] Y. J. Guo and X. R. Wu, "Bridging stress distribution in center-cracked fiber reinforced metal laminates: modeling and experiment", *Eng. Fract. Mech.* **63**:2 (1999), 147–163.

[Iarve and Pagano 2001] E. V. Iarve and N. J. Pagano, "Singular full-field stresses in composite laminates with open holes", *Int. J. Solids Struct.* **38**:1 (2001), 1–28.

[Lekhnitskiĭ 1981] S. G. Lekhnitskiĭ, *Theory of elasticity of an anisotropic body*, Mir, Moscow, 1981. MR 82d:73001

[Marissen 1988] R. Marissen, *Fatigue crack growth in ARALL: a hybrid aluminum-aramid composite material–crack growth mechanisms and quantitative predictions of the crack growth rates*, Ph.D. thesis, Delf University of Technology, The Netherlands, 1988.

[Muskhelishvili 1953] N. I. Muskhelishvili, *Some basic problems of the mathematical theory of elasticity. Fundamental equations, plane theory of elasticity, torsion and bending*, P. Noordhoff Ltd., Groningen, 1953. MR 15,370d

[Pagano 1978] N. J. Pagano, "Stress fields in composite laminates", *Int. J. Solids Struct.* **14**:5 (1978), 385–400.

[Ritchie et al. 1989] R. O. Ritchie, W. Yu, and R. J. Bucci, "Fatigue crack propagation in ARALL laminates: measurement of the effect of crack-tip shielding from crack bridging", *Eng. Fract. Mech.* **32**:3 (1989), 361–377.

[Roebroeks 1994] G. H. J. J. Roebroeks, "Fibre-metal laminates: recent developments and applications", *Int. J. Fatigue* **16**:1 (1994), 33–42.

[Tsai and Hahn 1980] S. W. Tsai and H. T. Hahn, *Introduction to composite mechanics*, Technomic, Lancaster. PA, 1980.

[Whitney 1987] J. M. Whitney, *Structural analysis of laminated anisotropic plates*, Technomic, Lancaster, PA, 1987.

[Wu and Cheng 1999] X. J. Wu and S. M. Cheng, "A higher-order theory for plane stress conditions of laminates consisting of isotropic layers", *J. Appl. Mech.* (*Trans. ASME*) **66** (1999), 95–100.

[Zhang et al. 2002] Z. Zhang, J. Laliberté, X. J. Wu, and C. Poon, "Generating da/dN curves", Progress Report LM-SMPL-2002-0191, Structures, Materials and Propulsion Laboratory, Institute for Aerospace Research, National Research Council of Canada, 2002.

Received 10 Oct 2005.

XIJIA WU: xijia.wu@nrc-cnrc.gc.ca
Structures and Materials Performance Laboratory, Institute for Aerospace Research, National Research Council of Canada, 1200 Montreal Road, M-13, Ottawa, ON K1A OR6, Canada

ZHONG ZHANG: Zhong.Zhang@nrc-cnrc.gc.ca
Department of Mechanical and Aerospace Engineering, Carleton University, 1125 Coloniel By Drive, Ottawa, ON K1S 5B6, Canada

J. LALIBERTÉ: Jeremy.Laliberte@nrc-cnrc.gc.ca
Structures and Materials Performance Laboratory, Institute for Aerospace Research, National Research Council of Canada, 1200 Montreal Road, M-13, Ottawa, ON K1A OR6, Canada